Experimental Study on Thermal Fatigue Life Prediction Model of PBGA Solder Joints

Jiang Shao
Equipment Service Product Department
China Aero Polytechnology Establishment
Beijing, China

***Abstract*—In the Prognostics and Health Management (PHM) technology of airborne products, the accuracy of life prediction model is very important for the life prediction. In order to acquire the proper life prediction model, the thermal fatigue life prediction model of PBGA solder joints was validated and modified by combining thermal cycle reliability experiment with finite element analysis. Firstly, during the thermal cycle reliability experiment, the resistance values of solder joints on test samples were surveyed and collected in real time, and the characteristic failure time of PBGA solder joints were obtained by Weibull probability distribution. Subsequently, the finite element analysis model of the PCB test sample was established based on the ABAQUS software, and Anand model was used to simulate the visco-plastic constitutive relationship of the solder joints, thus we can obtain the stress and strain data of the key solder joints, and the thermal fatigue life was calculated based on the Engelmaier model. Finally, the model parameters were modified by comparing the experimental results with the simulation results.**

Keywords- PBGA; life prediction model; reliability; thermal cycle test; finite element analysis

I. INTRODUCTION

In electronic packaging devices, solder joints are used to achieve the electrical and mechanical connections between each parts. With the great improvement of circuit integration, the numbers of solder joints are increasing and the sizes are decreasing, and Plastic Ball Grid Array (PBGA) packages are widely used in aeronautics and astronautics areas.

During the usage period of the airborne electronic products, temperature is always the most important influence factor to the reliability, and different kinds of solder joints are often the weakest parts in the products. Researches show that 55 percent of electronic package failure is caused by temperature, and most of them are solder joint failures [1]. Therefore, the life prediction of solder joints under thermal loading condition is an important issue in the design and manufacture of electronic packaging are. Under the thermal cycle loading condition, thermal expansion coefficient of each component material does not match each other, which will result in alternating thermal stress and inelastic strain in solder joint, thus the damage will accumulate gradually and the micro-cracks in the solder joint will initiate and propagate, finally lead to the final failure of the electronic package.

At present, the fatigue life of solder joints under thermal cycling loading condition has been studied extensively at home and abroad. Coffin and Manson [2, 3] proposed that plastic deformation was the main failure cause of solder joints, and they established the famous Coffin-Manson fatigue life model, but this model neglected the influences of temperature change rate and temperature amplitude. Engelmaier [4, 5] modified the Coffin-Manson model by introducing the thermal cycling frequency, cycling temperature and elastic-plastic strain of thermal cycling loading into the model, and proposed the Engelmaier model. Now Engelmaier model is still widely utilized to calculate the thermal fatigue life of solder joints for electronic products in engineering.

In order to verify if the Engelmaier model is available to the domestic electronic products, this paper studies the thermal fatigue life prediction model of PBGA solder joints through thermal cycling experiments and finite element analysis, and the Engelmaier model parameter was verified to assure the prediction accuracy.

II. THERMAL CYCLE EXPERIMENTS

A. Test Sample Design

The test samples are three printed circuit boards (PCB) with 12 PBGA packages, they are symmetrically distributed on the board, and the distance between the horizontal packages is 10 mm. The sizes of the sample are 300 mm x 180 mm x 2 mm. Four fixed holes are designed at four corners, the structure of the test sample is shown as Fig. 1.

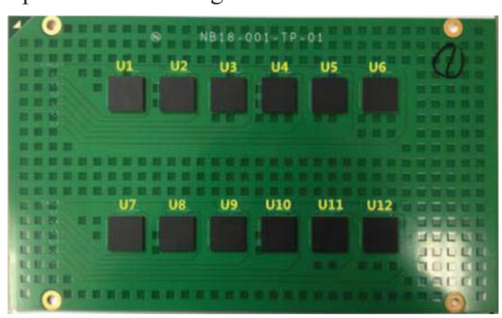

Figure 1. Test sample

As shown in Fig. 2, according to IPC-7095C [6], the size of PBGA package is 21 mm*21 mm, the diameter and pitch of solder ball is 0.5 mm and 1.0 mm individually, the number of solder balls is 256 and the material is Sn63Pb37. In order to monitor the resistance values of the solder joints, chrysanthemum chain circuit is designed in the sample, and the circuit diagram is shown as Fig. 3. The cracks in solder joints will cause resistance fluctuation during the thermal cycle

978-1-7281-0860-5/19/$31.00 ©2019 IEEE

experiment [7], and we can monitor the solder joint failure accordingly. Keithly 2750 data acquisition system is used here to monitor the chrysanthemum chain circuit in real time.

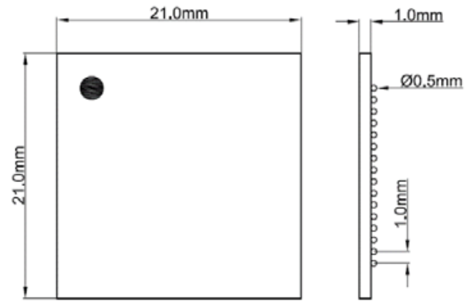

Figure 2. Geometric dimensions of pbga packaging chips

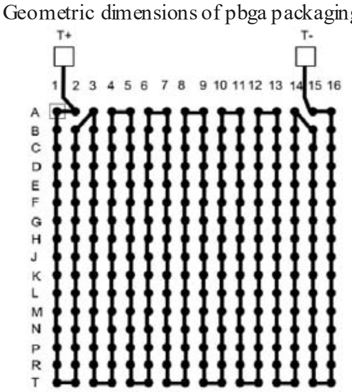

Figure 3. Circuit diagram of chrysanthemum chain formed by solder joint and PCB board

B. Experimental Condition

As shown in Fig. 4, three test samples were fixed on the fixture by bolts, and the fixture was put into the EVH49-2-30-wc-ln2-X temperature test chamber. The experimental conditions are designed according to JESD22-A104D[8] standard as shown in Table 1.

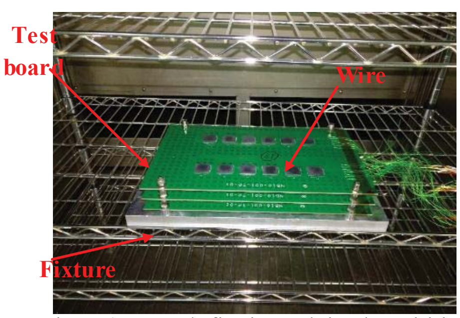

Figure 4. Sample fixation and signal acquisition

TABLE I. THERMAL CYCLE EXPERIMENTAL CONDITIONS

Temperature range	Increasing and Decreasing Temperature Rate	Temperature residence time	Cycle period
-55 ℃~ 125 ℃	15 ℃/min	15 min	54 min

III. EXPERIMENTS RESULTS

During each thermal cycle, the relationships between the average resistance (including line resistance, contact resistance and device resistance) and the number of thermal cycles are shown as Fig. 5. The resistance value varies with the change of temperature, and the resistance value of the circuit is different at high and low temperatures. Therefore, when judging the failure, it is necessary to compare the resistance values at the same temperature. If the resistance changes more than 20%, the failure of solder joints can be judged.

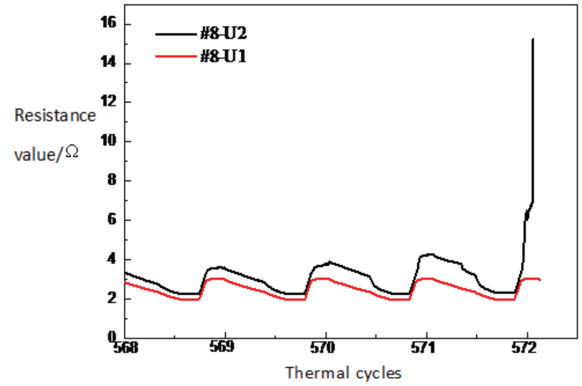

Figure 5. #8-U2 resistance change curve during the experiment

Weibull distribution is widely used in life experiments of various semiconductor devices. During the experiment, the failure time is monitored in real time. After the failure time of each device is obtained, two-parameter Weibull probability distribution is used to process the failure time.

$$F(t) = 1 - \exp[\ (t/\alpha)^{\beta}\ ] \tag{1}$$

Where, t is the failure life, $F(t)$ is the probability when the life is not greater than t, α is the characteristic failure time, and β is the shape parameter or Weibull slope.

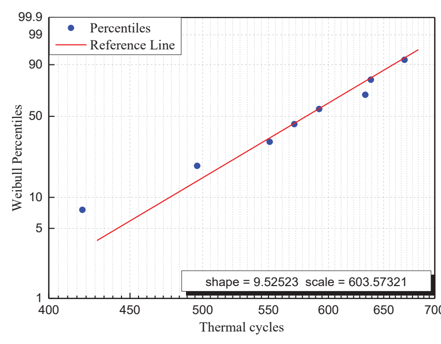

Figure 6. Weibull probability diagram of experimental samples

As shown in Fig. 6, the characteristic failure time α is 604 cycles and the shape parameter β is 9.53.

IV. FINITE ELEMENT ANAYSIS

A. Finite Element Model

In this paper, we use the commercial software ABAQUS to establish the finite element model (FEM) of the PCB test sample. In order to enhance the analysis efficiency and improve the analysis speed, we simplify the FEM by several means: (1)

ignoring the printed copper wires on the board; (2) no residual stress and strain are considered; (3) ignoring the influence of welding resistance layer; (4) ideal connection between materials, no voids or impurities; (5) all materials are isotropic. (6) The other pads and solder joints of 11 chips are simplified into a layer of uniform medium respectively, as shown in Fig 7. The simplified analysis models include: plastic sealing material (EMC), substrate (BT), solder ball, printed circuit board (PCB), pad, simplified pad layer and simplified solder joint layer. The FEM element types include C3D8R and linear C3D6, as shown in Fig 8.

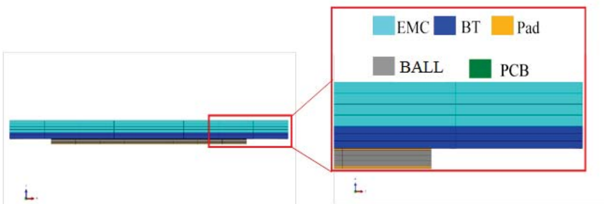

Figure 7. Simplified chip finite element model

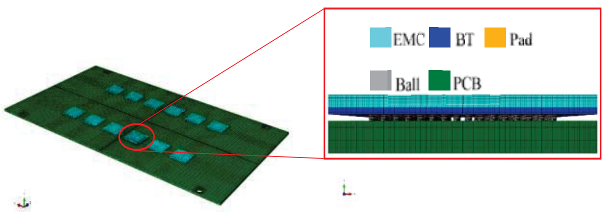

Figure 8. Finite element model of the test sample

B. Material Parameters

The melting point of the material Sn63Pb37 is 218 ℃, the ratio of its actual temperature to theoretical melting point temperature is larger than 0.5, thus creep is dominant in inelastic strain [9]. Anand constitutive model is used to analyze the mechanical behavior of the PBGA solder joints, and the parameters are shown in Table 2. Other materials in the model are set as uniform linear elasticity. Considering the influence of temperature on material properties, the reference temperature is 125 ℃. The material parameters of each component in the model are listed in Table 3.

TABLE II. ANAND MODEL PARAMETERS OF SN63PB37 [10]

Definition	Symbol	Unit	Value
Initial deformation impedance value	s_0	MPa	56.63
Viscoplastic deformation activation energy	$Q{\cdot}k^{-1}$	K	10830
Exponential coefficient	A	s^{-1}	1.49E7
Stress parameter	ξ	-	11
Strain rate sensitivity exponent of stress	m	-	0.303
Deformation impedance saturation value coefficient	$\hat{s}$	MPa	80.415
Strain hardening and softening constant	h_0	MPa	2640.75
Strain rate sensitivity exponent of deformation impedance saturation value	n	-	0.0231
Strain rate hardening sensitivity exponent related to hardening/softening	a	-	1.34

TABLE III. MATERIAL PARAMETERS OF EACH COMPONENT IN THE PACKAGE

Parts	Reference Temperature /℃	Elastic Modulus /MPa	Poisson Ratio	Coefficient of thermal expansion /1e-6/℃
Sn63 Pb37	-55	47970	0.352	24.1
	-35	46890	0.354	24.6
	-15	45790	0.357	25.0
	5	44380	0.360	25.2
	22	43250	0.363	25.4
	50	41330	0.365	26.1
	75	39450	0.370	26.7
	100	36850	0.377	27.3
	125	34590	0.384	27.9
SMF	—	4137	0.4	80.8
PCB	—	48200	0.3	20
EMC	—	14210	0.3	13.8
BT	—	22000	0.28	18
Pad	—	129000	0.38	16.9

C. Boundary Conditions and Loads

According to the fixed condition of the test sample, the four bolt holes of the FEM are fully constrained as shown in Fig. 9.

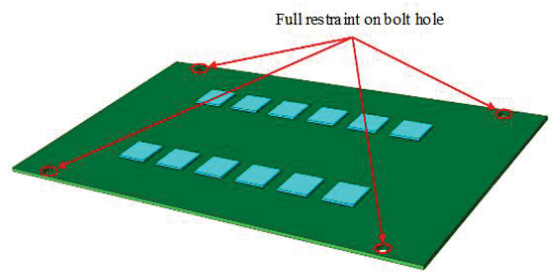

Figure 9. Boundary conditions

According to the experimental loading conditions, the temperature cycle profile used in finite element analysis is shown as Fig. 10. The temperature range of the thermal cycle is 180℃ (-55℃ to 125 ℃), the heating and cooling time are 12 minutes, the residence time of high and low temperature are 15 minutes, the heating and cooling rate is 15℃ per min, and the cycle frequency f is 0.9 cycle per hour. Four cycles are loaded sequentially, and the total duration is 12960 s. Visco analysis step is used for calculation in ABAQUS.

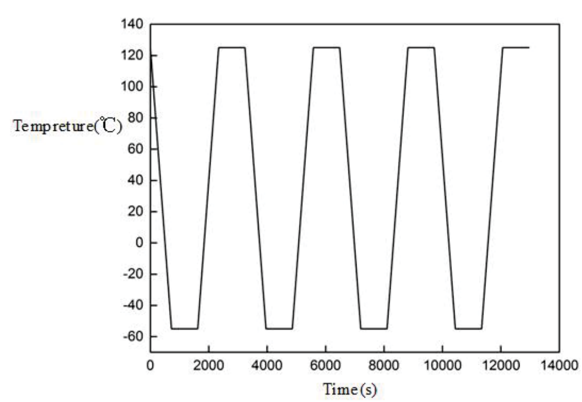

Figure 10. Thermal cycle load curve

D. *Results Analysis*

In the reliability analysis of solder joints, creep strain is generally used to link with the thermal fatigue life [11]. The equivalent creep strains of solder joints are analyzed as Fig 11. The maximum equivalent creep strains occur at the corner positions which is located near the packaging side. Thus the solder joints in the corner position are easy to fail and they can be considered as the dangerous solder joints.

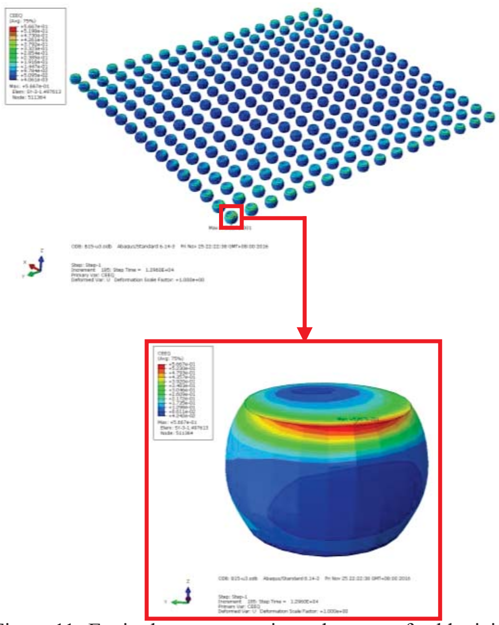

Figure 11. Equivalent creep strain nephogram of solder joint

The von-Mises stress of dangerous solder joints varies with the temperature cycle as shown in Fig. 12. We can see the von-Mises stress varies periodically with the temperature cycle, the maximum stress in each cycle occurs in the low temperature residence stage, and the stresses in this stage are relatively high. During the whole residence period, obvious stress relaxation effects appear in the solder joints.

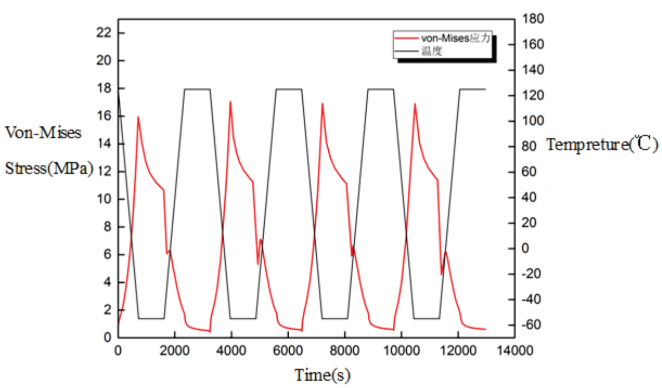

Figure 12. Variation of von-Mises stress with thermal cycle

Fig. 13 shows the variation of inelastic shear strain with temperature cycle of dangerous solder joints. The inelastic shear strains of these solder joints also change periodically with the temperature cycle, and the amplitudes increase gradually. During the cooling stage, the non-elastic shear strains increase rapidly due to the creep deformation of the solder joints. During the low-temperature residence stage, the creep deformations of the solder joints are not obvious, so the non-elastic shear strains change slowly. During the heating stage, the non-elastic strains of the solder joints decrease sharply due to the decrease of the elastic modulus of solder joints, and during the high-temperature residence stage, the inelastic shear strain decreases slowly due to the creep deformations in those solder joints.

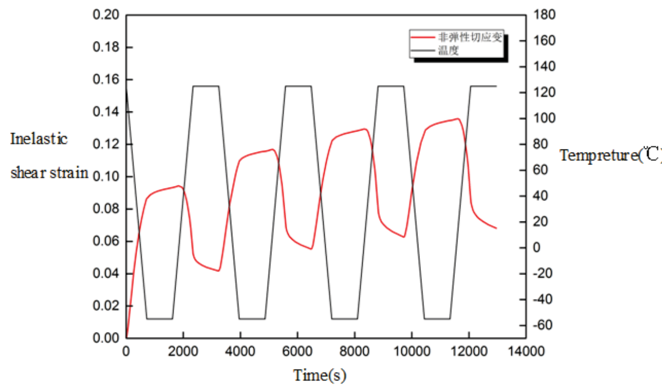

Figure 13. The variation of inelastic shear strain with temperature

V. THERMAL FATIGUE PREDICTION MODEL

The thermal fatigue life of solder joints can be calculated using the Engelmaier model [4,12]:

$$N_f = \frac{1}{2}\left(\frac{\Delta\gamma_\tau}{2\varepsilon'_f}\right)^{\frac{1}{c}} \tag{2}$$

Where, N_f is the fatigue life, $\Delta\gamma_\tau$ is the total shear strain range, ε_f is fatigue ductility coefficient which is a constant related to the material of solder joint, and c is fatigue ductility exponent which can be calculated as:

$$c = -0.442 - 0.0006T_{sj} + 0.0174\ln(1+f) \tag{3}$$

Where, T_s is the mean cyclic temperature and f is the frequency of cycles per day.

Using the inelastic shear strain of the fourth temperature cycle in Fig.13, the inelastic shear strain amplitude of dangerous solder joints $\Delta\gamma_\tau$ is obtained as 0.084. According to the experimental results of thermal cycle, the characteristic failure time (the failure time when the cumulative failure probability of the sample reaches 63.212%) is taken as the fatigue life N_f, and it is 604 cycles. Thus the thermal fatigue life prediction model in the test can be established as:

$$N_f = \frac{1}{2}\left(\Delta\gamma_\tau/1.49\right)^{-1/0.4052} \tag{4}$$

VI. SUMMARY

Engelmaier model is widely utilized to calculate the fatigue life of solder joints in electronic products which are often working under the thermal cycling loading condition. In this paper, thermal cycle experiment and finite element analysis are conducted on PCB samples, the resistance of solder joints are monitored in time to obtain their failure time, and the stress and strain data of key solder joints are obtained by finite element analysis. By comparing the experimental results with the FEA simulation results, the model parameters of Engelmaier model are determined.

REFERENCES

[1] Luan J E, Tee T E, Pek E. Advanced numerical and experimental techniques for analysis of dynamic responses and solder joint reliability during drop impact [J]. IEEE Transactions on Components and Packaging Technologies. 2006, 29(3): 449-456.

[2] L.F. Coffin, Jr. A study of the effects of cyclic thermal stresses on a ductile metal. Transactions American Society of Mechanical Engineers, vol. 76, pp. 931-950, 1954.

[3] S.S. Manson. Fatigue: a complex subject-some simple approximation, Experimental Mechanics. vol. 5, pp. 193-226, 1965.

[4] W. Engelmaier. Fatigue life of leadless chip carrier solder joints during power cycling. IEEE Transaction on Components, Hybrids, and Manufacturing Technology, vol. CHMT-6, pp. 232-237, 1983.

[5] W. Engelmaier, A. Attarwata. Surface-mount attachment reliability of clip-leaded ceramic chip carrier on FR-4 circuit boards. IEEE Transaction on Components, Hybrids, and Manufacturing Technology, vol. 12, pp. 284-296, 1989.

[6] IPC-7095C. Design and assembly process implementation for BGAs. IPC-Association Connecting Electronics Industries. 2013: 12-71.

[7] Yu D, Al-Yafawi A, Park S, Chung S. Finite element based fatigue life prediction for electronic components under random vibration loading[C]. Proceedings-Electronic Components and Technology Conference. Las Vegas. 2010: 188-193.

[8] JESD22-A104D. Temperature Cycling. JEDEC Solid State Technology Association, 2009, 5.

[9] Wang Qiang, Liu Yong, Liang Lihua. Anand parameter determination and CSP solder joint life prediction of lead-free SnAgCu [J]. Engineering Mechanics, 2009, 26 (10): 177-182. (In Chinese)

[10] Li Yang. Reliability simulation and experimental study of BGA solder joints for hybrid assembly [D]. Harbin University of Technology, 2013. (In Chinese)

[11] Pecht M, Lall P. The Influence of Temperature on Integrated Circuit Failure Mechanisms [J]. Quality and Reliability Engineering International, 1992(8): 167-175.

[12] Ren Chao, Shao Jiang, Zeng Chenhui, Xue Ping. Impact analysis of pin structure interconnection reliability of SOP devices [J]. Mechanical strength, 2016, 38 (3): 591-595. (In Chinese)